KEK
Insight through Accelerators.

Inter-University Research Institute Corporation
High Energy Accelerator Research Organization (KEK)

Photon Factory Hybrid Light Source
(PF-HLS)

Conceptual Design Report (CDR) ver. 1

Table of Contents

1. Overview of PF-HLS

Mission and Concept

Considering the fundamental philosophy of KEK, which was established to contribute to the development of accelerator science as a research institution open to the world, and the role of the Inter-University Research Institute Corporation in Japan, a country with numerous operational synchrotron radiation facilities, the Photon Factory (PF) proclaims its mission as follows:

1. To supply new technologies and foster young talent leading the world in synchrotron radiation science through research and development
2. To promote diverse research on materials and life as an advanced infrastructure facility

The PF Hybrid Light Source (PF-HLS), proposed by the PF established in 1982, aims to continue fulfilling its missions and contributing to society. KEK has been driving the PF-HLS project, intending to position Japan as a leader in material and life sciences for the next 100 years.

The concept of PF-HLS is to be a 'synchrotron radiation multibeam experimental facility' that enables the integration of all aspects of synchrotron radiation performance. This integration advances the "deepening," "fusion," and "creation" of research fields and methods, making it possible to achieve the scientific goal of "elucidating the origins of functions in materials and life." Scientific exploration based on free and prosperous individual ideas is essential for utilizing the Inter-University Research Institute Corporation, which has pioneered academic research.

Therefore, the PF-HLS is envisioned as a facility that significantly enhances the diversity and freedom in hardware (such as light-source accelerators and beamlines) and software (facility operations). The PF-HLS has a hybrid light source comprising an energy-switchable storage ring and a superconducting linac. While various synchrotron radiation facilities share a wide wavelength range covering vacuum ultraviolet (VUV), soft X-rays (SX), and hard X-rays (HX), the storage (SR) beam provided by the 2.5/5.0 GeV switchable storage ring covers most of the VUV, SX, and HX with a single source. The superconducting linac also supplies a single-pass (SP) beam with a femtosecond pulse width that is unattainable by the storage ring. At the PF-HLS, we will develop SR single-beam, SR + SR multibeam, and SR + SP multibeam experiments in the 40–50 beamlines (Figure 1-1).

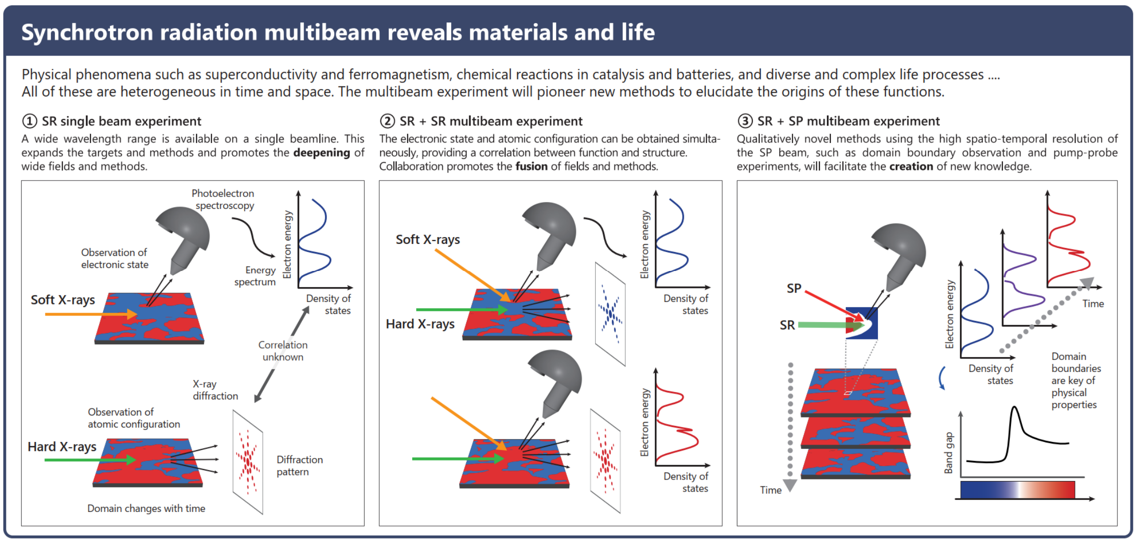

Figure 1-1: Concept of the PF-HLS.

Implementation and Operation

The PF-HLS project is led by the Inter-University Research Institute Corporation KEK. Positioned as the next-generation facility succeeding the current storage rings (PF and PF-AR), this project realizes the new synchrotron light-source facility outlined in the KEK Roadmap 2021 and the KEK Project Implementation Plan 2022, formulated with advice from the KEK Science Advisory Committee. Inside KEK, the Institute of Materials Structure Science and Accelerator Laboratory will play a pivotal role in implementation and operation. Externally, cooperation will be obtained from UVSOR and HiSOR, which are part of the Synchrotron Radiation Academic Infrastructure Network formed in 2019 in response to a request from the Japan Society for Synchrotron Radiation Research, as well as from PF-UA, the user association of PF. The involvement of these entities will be further evaluated, along with the efforts to expand their engagement with new domestic and international partners.

A facility characterized by high diversity and freedom allows for experimental approaches involving trial and error, innovative experiments with developmental aspects, and long-term experiments. This aids the exploration of research frontiers and significantly contributes to nurturing talent. Participation in the construction and advancement of new types of facilities, which is unprecedented worldwide, also contributes substantially to the development of facility personnel. Establishing an appropriate utilization system is essential to fully leverage the diversity and freedom of the PF-HLS. A diverse and free yet simple utilization system will be established through discussions with the PF Program Advisory Committee (PF-PAC), which comprises more than half of its members from outside KEK.

The ideal plan for the annual schedule and construction sites is shown in Figure 1-2. As numerical targets, we aim to "increase the number of users by 50–100%" and "achieve a 10% increase in operating hours and a 25–35% decrease in power consumption" compared to the current facilities (PF and PF-AR).

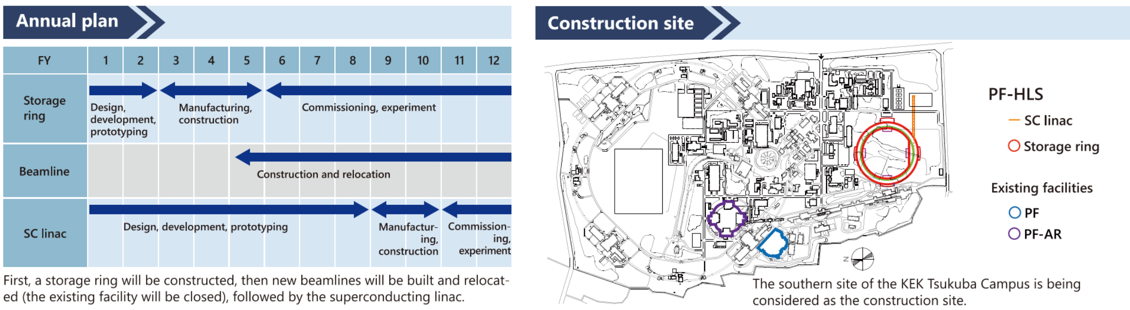

Figure 1-2: Annual plan for the PF-HLS (left) and proposed construction sites (right).

Examples of the science to be conducted at the PF-HLS, the necessary beamline technology, and information on the source accelerator are detailed in Chapters 2, 3, and 4, respectively. A brief introduction of the content is given below.

Science (Chapter 2)

We introduce science cases that become possible through the deepening, fusion, and creation of research fields and methods aimed at the scientific goal of elucidating the origins of functions in materials and life. At the PF-HLS, a wide wavelength range can be utilized in a single beamline, owing to the 2.5/5.0 GeV switchable feature. By leveraging this characteristic, the SR single-beam experiments can advance deepening across various fields and methods. In the SR + SR multibeam experiments, the fusion of different fields and methods is facilitated through collaborative approaches. In the SR + SP multibeam experiments, the high temporal and spatial resolutions of SP beams can enable the creation of unprecedented fields and methods.

Beamlines (Chapter 3)

We discuss beamline technology for SR single-beam experiments, including switching optical elements over a wide wavelength range and removing higher-order harmonics. Regarding the SR + SR multibeam experiments, we explain the technology required for position control for the simultaneous exposure of two beams. For SR + SP multibeam experiments, we describe the precise control of the optical path length and timing characteristics of the detectors to fully utilize the high temporal and spatial resolution of SP beams. Technological developments and proof-of-concept experiments are conducted in the wide-wavelength-range SX beamline BL-12A and the multifunctional research and development beamline BL-11A and -11B, which are currently under construction at the PF.

Light-Source Accelerators (Chapter 4)

The source accelerator comprises a 2.5/5.0 GeV switchable storage ring and a superconducting linac [1]. In this CDR, we primarily describe the storage ring with the aim of early construction (Figure 1-2). The storage ring is designed with multiple 10 m and 5 m straight sections, allowing the placement of a couple of insertion devices (IDs) in the same straight section. In principle, a wide wavelength range from 10 to 100 keV can be covered using a single beamline (Figure 1-3). The large switch between 2.5/5.0 GeV is unprecedented globally, and we are advancing technological development and proof-of-concept experiments, including machine studies at PF and PF-AR.

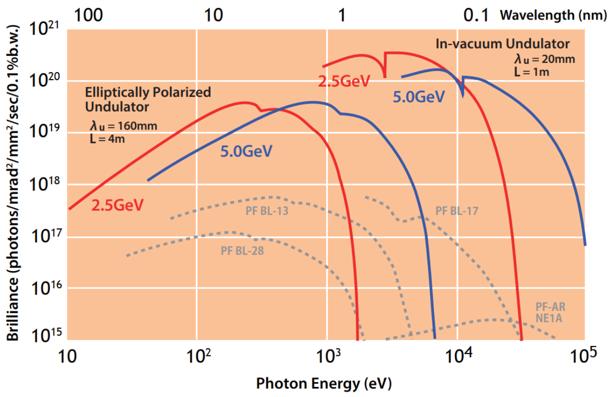

Figure 1-3: Example of the energy spectra at the PF-HLS.

[1] K. Harada *et al.*, *J. Synchrotron Rad.* **29**, 118 (2022).

2. Science

2-1. Deepening Magnetic Thin-Film Research through Element-Selective Structural and Magnetic State Analysis

Magnetic thin films exhibit unique magnetic states such as perpendicular magnetic anisotropy. When adequately stacked with different films, including non-magnetic films, they demonstrate intriguing phenomena such as giant magnetoresistance and exchange bias effects, which are applied in spintronics technology. A definite origin of these unique phenomena is the distinct atomic arrangement (structure) in nanometer-scale thin films, which differs from that in bulk materials. While the structure and magnetism of thin films have been studied using various methods, the magnetism exhibited by thin films can change significantly owing to slight differences in the structure and chemical state. Therefore, the observation of the structural and magnetic states of the same sample is crucial. Magnetic thin films comprise many elements, and understanding their magnetism requires element-selective observation of the magnetic moments of each constituent element.

At PF-HLS, the switch between 2.5 GeV and 5.0 GeV allows the use of a wide range of X-ray energies with a single beamline and a single measurement device, enabling the observation of the structure and magnetic state of the same sample. The energy range and measurement methods covered by a 56-mm period APPLE-II-type undulator are shown in Figure 2-1-1. EXAFS (using linear polarization) allows the element-selective determination of bond distances and other structural parameters in each layer of stacked thin films comprising different elements. This provides structural information that is directly linked to the emergence of unique magnetism, such as lattice matching/mismatch at interfaces and the resulting structural distortions. Because of its elemental selectivity and polarization dependence, this method can be used to distinguish and analyze the vertical and in-plane directions of films. The K-absorption edges of 3d transition metals and the L-absorption edges of 4d and 5d transition metals, which are the major components of magnetic thin films, lie between approximately 2 and 12 keV and are suitable for EXAFS measurements. For magnetic state analysis, XMCD (using circular polarization) and XMLD (using linear polarization) are highly effective and offer elemental selectivity. The L-absorption edges for 3d and 4d transition metals and the M-edges for rare-earth elements, which are suitable for direct observation of the orbitals related to magnetism, lie in the range of a few hundred electron volts to 4 keV. M-edges for 5d transition metals (2–3 keV) are also accessible. Consequently, this comprehensive approach for studying the structure and magnetic states across almost all elements in magnetic thin films can reveal their unique magnetism, substantially deepening the field of magnetic thin-film research.

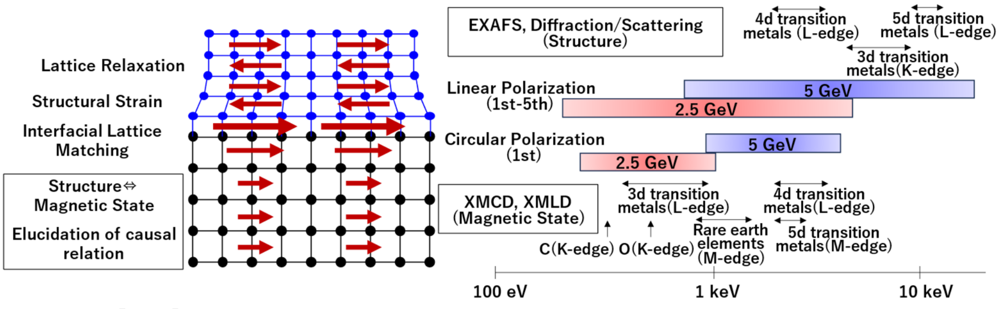

Figure 2-1-1: [Left] Schematic of the structure and magnetism in magnetic thin films. Unique magnetism arises due to lattice matching/mismatch and structural distortions at the interface, caused by growing thin films with different lattice constants compared to the substrate. [Right] Relationship between the energy covered by the 56-mm period APPLE-II-type undulator, target elements, and measurement methods.

2-2. Deepening Liquid and Glass Structure Studies through Broad Wavenumber Range Scattering and Electronic State Observation

The properties of liquids and glasses are closely related to their structures. In geoscience, understanding the properties of silicate magmas and aqueous fluids that incorporate various incompatible elements (those that are difficult to incorporate into crystals) is critical. In materials science, interest lies in the structures of various types of glasses with a wide range of compositions, such as functional glasses with different elemental additives and metallic glasses. Although liquids and glasses are often considered disordered and structureless, they frequently exhibit short-range structures around certain atoms (unit structures) and intermediate-range structures formed by the bonding of these units. These relatively short-scale structures are revealed by scattering information that extends to high-wavenumber regions. Conversely, in cases where immiscible compositions mix or phase separation occurs with partial crystallization, heterogeneous structures emerge, reflecting the interfacial energies. These structures are typically observed as scattering information in the low-wavenumber (small-angle) regions. Furthermore, considering the ability of liquids and glasses to incorporate various elements, a more detailed structural determination can be expected by combining element-selective measurements such as XAFS and anomalous (resonance) scattering, which can extract electronic and structural information of the elements of interest. However, reproducing sample states is not invariably easy because of their high melting points, compositional instability due to evaporation, and relatively long structural relaxation times. In such cases, measurements performed at the same beamline under identical conditions are desirable.

At the PF-HLS, the use of an in-vacuum undulator enables the utilization of X-rays ranging from 4 to 100 keV at 5.0 GeV, which allows for small-angle and total scattering measurements that have been conducted thus far. Additionally, X-rays ranging from 1 to 4 keV become available by switching to 2.5 GeV. This region includes the K-absorption edges of elements, such as Na, Mg, Al, Si, P, S, Cl, Ar, K, and Ca, which are abundant on the Earth's surface and are important in geoscience and materials science. However, the coordination numbers and valences in liquids and glasses for these common elements are not consistently evident, and the relationship between their electronic states/structures and macroscopic properties such as viscosity, glass transition temperature, and strength should be elucidated in the future. Furthermore, the observation of the L- and M-absorption edges of 4d transition metals and rare-earth elements, respectively, in this energy range potentially deepens the understanding of the partitioning behavior of incompatible elements and the origin of their functionalities in glasses. Thus, broad-wavenumber-range scattering and electronic state observation are expected to deepen research on the structures of liquids and glasses significantly.

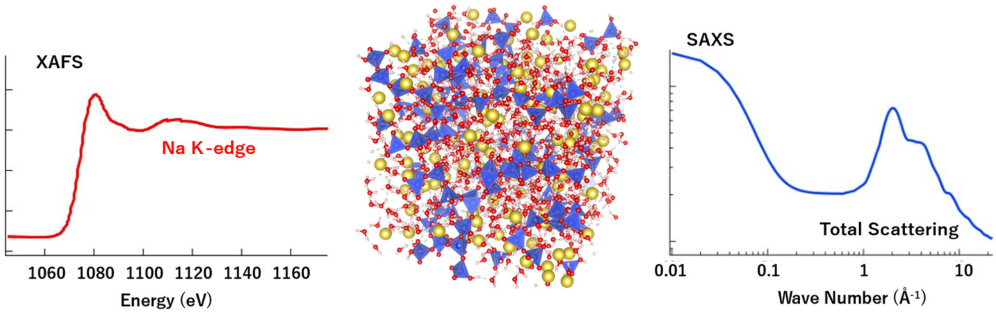

Figure 2-2-1: Example of research on the structure of liquids and glasses through simultaneous measurement using element-selective methods and broad-wavenumber-range scattering. Liquids and glasses can incorporate various elements. The electronic and coordination states of each element are crucial in manifesting functionality and are related to structures at various scales.

2-3. Fusion of Synchrotron Radiation Irradiation and Measurement Techniques for Advanced Radiation Therapy

The three principal treatments for cancer includes surgery, chemotherapy, and radiation therapy. In radiation therapy, killing cancer cells by radiation and minimizing the damage to the surrounding normal cells are crucial. As a result, to achieve this, various radiotherapies have been proposed and put into practical use, such as concentrating the dose on the tumor, leveraging the biological differences between cancerous and normal cells, and combining these approaches. For instance, ultra-high-dose-rate irradiation (FLASH radiotherapy), which involves short-duration irradiation at a dose rate over a thousand times higher than that of conventional radiation therapy, has garnered attention. In FLASH radiotherapy, while the tumor response (therapeutic effect) remains similar to typical dose rates, the damage to normal tissues is reduced. The prevailing theory behind this method is that high dose rates generate high-density radicals, leading to oxygen depletion, thereby suppressing DNA damage in normal cells, whereas tumors, which are typically oxygen-deprived, are less affected. However, research into the radiochemical mechanisms of this method is still in its infancy.

Synchrotron radiation, with its ability for element-selective irradiation using the absorption edges of biological constituent elements and site-specific irradiation using microbeams, is an excellent light source capable of controlling the initial processes of radiobiological effects. This provides various insights that contribute to the advancement of radiation therapy. Previously, the focus was mainly on observing reactions occurring from several tens of minutes to several days after irradiation using biochemical and biological methods. However, as is evident in the case of FLASH radiotherapy, reactions occurring on a shorter timescale, from energy deposition by radiation to radical formation and biomolecular damage, significantly influence the final biological effects. These short-timescale reactions, which have been under-researched, occur spatially and temporally heterogeneously in inhomogeneous cells and tissues and can be detected by many measurement techniques using synchrotron radiation as a probe.

At the PF-HLS, fusing the synchrotron radiation irradiation and biological sample environment techniques that have been cultivated with synchrotron radiation measurement techniques enable simultaneous irradiation of the samples and observation of subsequent radiochemical reactions. Furthermore, the use of high-energy X-rays through 2.5/5.0 GeV switching opens the possibility of expanding research into conditions closer to actual radiation therapy with thicker samples, such as 3D cultures and animals.

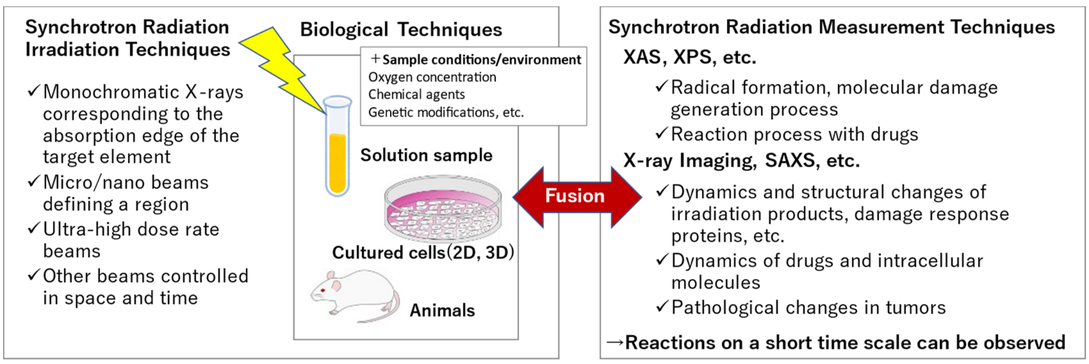

Figure 2-3-1: Fusion of synchrotron radiation irradiation, biological sample environment, and synchrotron radiation measurement techniques. By observing reactions on shorter timescales, the aim is to elucidate the mechanisms of radiobiological effects, contributing to the advancement of radiation therapy.

2-4. Fusion of Measurement Methods for Correlational Studies on Structure and Function in Soft Materials

Represented by plastics, soft materials form hierarchical structures across a wide spatial scale ranging from nanometers to micrometers. The physical properties and functionalities of these systems are determined by complex spatial and temporal interactions at each hierarchical level. Unraveling the mechanisms underlying this inhomogeneous spatiotemporal hierarchical structure formation is crucial for enhancing the functionality of soft materials.

Soft materials comprise light elements, such as carbon, nitrogen, and oxygen, with carbon being pivotal in their molecular backbones and functional groups. In addition, ions such as Na, Mg, K, and Ca significantly influence their functionalities and properties. Small-angle X-ray scattering (SAXS) is suitable for evaluating structures at this broad spatial scale; however, distinguishing the spatial distribution of individual components is challenging. Anomalous SAXS (ASAXS), which utilizes the anomalous dispersion effect of elements, allows the assessment of the spatial distribution, bonding environment, functional groups, and orientation of these elements. For instance, using carbon-targeted ASAXS, the distribution of functional groups and various molecular frameworks can be distinguished through the chemical shift of carbon.

At the PF-HLS, the simultaneous use of two beams enables concurrent measurements using multiple previously challenging methods. For example, by using ASAXS with SX and X-rays in the several-kiloelectron-volt range, the spatial distribution of various carbon functional groups and the ions that govern their functionality and properties can be observed simultaneously. Concurrently, wide-angle X-ray Scattering (WAXS) provides information on the crystallinity and sub-nanometer-scale orientation. In addition to simultaneous SAXS/WAXS measurements for hierarchical structure evaluation, combining X-ray absorption spectroscopy (XAS) allows for operando observations during deformation, enabling tracking of dynamic changes in the structure and function. The use of two beams at the PF-HLS opens avenues for elucidating the complex correlation between the intricate hierarchical structures and functionalities of soft materials.

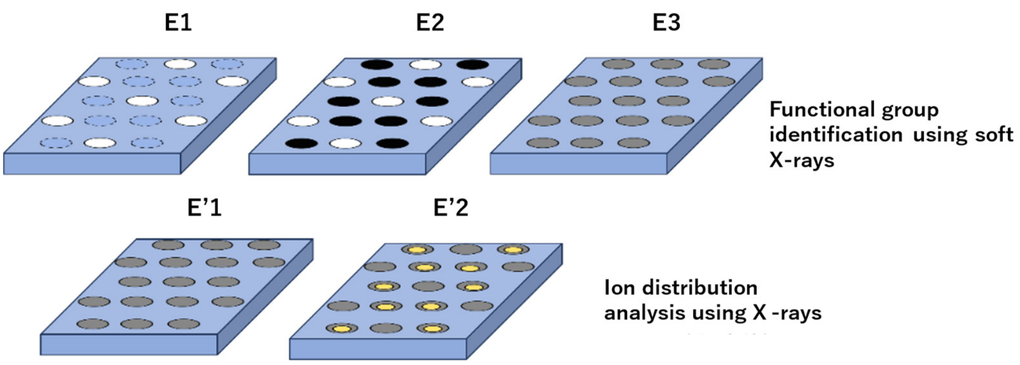

Figure 2-4-1: Example of multibeam SAXS measurement enabling functional group identification and ion distribution analysis. In soft materials with a sea-island structure, at X-ray energy E1, islands with a specific functional group (white) are observable. In contrast, at E2, two different islands with evident functional groups can be distinguished. At E3, the types of islands are indistinguishable. Additionally, using X-ray energy E'1, ion distribution cannot be discerned, but it is distinguishable at E'2. These combinations allow simultaneous knowledge of the spatial distribution of different functional groups and ions.

2-5. Creation of Photochemical Reaction Studies Integrating Spatiotemporal Scales

Photochemical reactions can facilitate reactions that are otherwise impossible to conduct under normal conditions. Therefore, understanding their mechanisms is not only of scientific interest but also an urgent task from a practical standpoint, such as utilizing solar energy for the photocatalytic generation of hydrogen and oxygen from water. Photochemical reactions begin with the light-induced excitation of electrons and the creation of holes, followed by processes such as electron and hole migration and the generation of active species, leading to the progression of chemical reactions accompanied by changes in spatial distribution. These processes evolve across various timescales, from femtoseconds to seconds, and spatial scales, from the atomic level to the micrometer scale. Light excitation typically occurs locally at the atomic scale. However, in chemical reactions, different chemical species often form domains at the nanometer to micrometer scale, and the reaction proceeds through the expansion, shrinkage, or movement of these domains. Reactions at the boundaries of these domains are crucial for the overall chemical reactions.

The PF-HLS aims to comprehensively study photochemical reactions by integrating spatiotemporal scales to understand the transitions in electronic states through photoexcitation, generation of active species, and their spatial movement leading to reactions. The simultaneous observation of the photoexcitation and relaxation processes on the femtosecond to picosecond timescale and the nanometer spatial scale, as well as the changes in the spatial distribution (domains) of elemental and chemical states on the microsecond to second timescale and the nanometer to micrometer spatial scale, are particularly important. This elucidates the interconnection of these aspects, from photoexcitation to chemical reactions.

For this purpose, wide-area imaging with a temporal resolution of milliseconds to seconds and spatial resolution of nanometers to micrometers, using SR beams (such as coherent imaging utilizing absorption edges and imaging microscope with photoelectrons or fluorescent X-rays), will track the spatial distribution of domains that change dynamically during reactions. Concurrently, focused SP beams of approximately 10 nm will be used for pump and probe measurements on the femtosecond to picosecond scale (such as XAS and photoelectron spectroscopy). For the first time, these simultaneous measurements will allow us to distinguish the parts (such as interior, exterior, and boundaries) and their corresponding domains in which the photoexcitation and relaxation processes observed with the SP beam occur. These domain-separated spatiotemporally resolved observations will create a new approach for photochemical reaction studies, enabling an integrated understanding of the entire process, from photoexcitation to chemical reactions, across broad spatiotemporal scales.

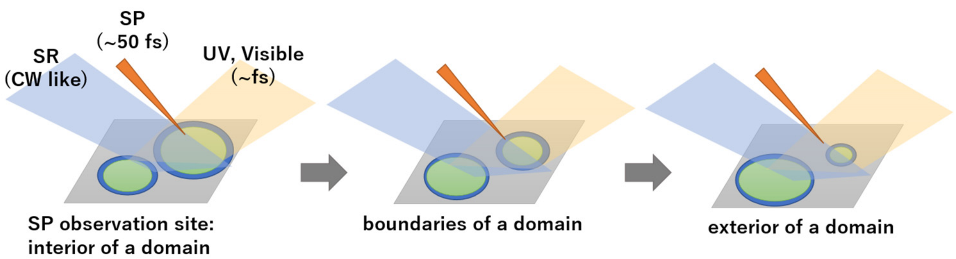

Figure 2-5-1: Schematic of the simultaneous use of SP and SR beams for integrated spatiotemporal scale observation of photochemical reactions. Photochemical reactions excited by UV or visible light (irradiated over the entire area) are observed simultaneously with the SP (ultrafast local probe) and SR (wide-area probe) beams. The excitation and relaxation processes are expected to differ within the interior, boundaries, and exterior of the domains, with the observation area of the SP beam changing dynamically due to the movement of the domains. The SR beam tracks the spatial distribution of the chemical states.

2-6. Creation of X-ray-Induced Phase-Transition Research Field

Phase transition phenomena in materials are of academic and practical importance because they involve changes in their physical properties and structure. This interest stems from the fundamental curiosity regarding the physical phenomena in which states are stabilized under external fields and the practical implications of these transformations.

In condensed matter systems, such as strongly correlated electron systems and molecular assemblies, the manifestation of diverse physical properties, such as electrical conductivity, magnetism, and dielectricity, is underpinned by the degrees of freedom of spins, orbitals, charges, and strongly coupled lattices within these systems. Measuring these ordered states is essential to elucidate the mechanisms underlying the emergence of these physical properties. In such systems, photoinduced phase transitions are proposed to start with photoexcited molecules, atoms, or ions that spread the photoinduced phase throughout the material. For example, phenomena in which a single photon induces phase changes at hundreds of sites have been reported. Furthermore, the large external field response, often observed in systems where multiple degrees of freedom are intricately intertwined, is apparently related closely to the coexistence of two phases near phase transitions, making coexistence and its temporal and spatial development focal points of interest. From this perspective, many measurements under phase control by external fields have been conducted, including pump-and-probe experiments using laser light as the pump and synchrotron or free-electron laser X-rays as the probe. Because synchrotron radiation can cover a wide energy range and selectively excite specific orbits, many examples of structural phase transitions induced by synchrotron light are known.

At the PF-HLS, where two synchrotron beams can be simultaneously irradiated as a pump and probe, unprecedented experiments to observe the temporal and spatial development of phase-transition behaviors will be possible. Focusing the SP beam on the nanometer scale allows the observation of the spatial development of phase transitions originating from this focal point using the SR beam on a scale from nanometers to micrometers. Concurrent time-resolved measurements will clarify the mesoscopic domain formation and propagation processes in photoinduced phase transitions. Techniques such as coherent imaging and multiscale SX microscopy, which are actively developed at the PF, will be utilized. In addition to observing the formation and propagation of distinctive phases such as skyrmions, using light vortices with angular momentum, as demonstrated at the PF, the use of synchrotron radiation for element- and orbital-selective excitation may also lead to the discovery of new types of phase transitions. The goal is to establish novel research on X-ray-induced phase transitions using two beams.

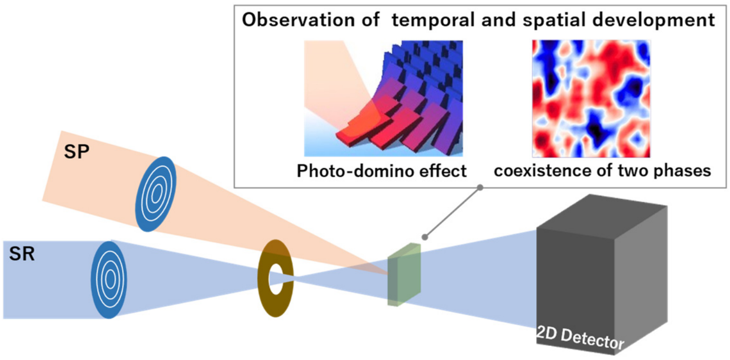

Figure 2-6-1: Example of observing the temporal and spatial development of a photoinduced phase formed by an SP beam using an X-ray microscope with an SR beam. The aim is to observe phenomena such as the changes in multiple molecules by a single photon (photo-domino effect) and the coexistence of two phases, which is predicted to be the origin of giant external field responses.

3. Beamlines

3-1. SR Single Beam

At the PF-HLS, the selection between 2.5/5.0 GeV allows a single beamline to access a wide range of wavelengths with high-brilliance light (SR beam). This section discusses beamline technologies for wide-wavelength-range utilization.

The configuration of the beamline optics is similar to that of the conventional setups for each wavelength range. However, covering a wide wavelength range within the same optical path requires switching between multiple optical elements and removing the higher-order light. Diffraction-grating monochromators covering a wide wavelength range are fabricated by switching between multiple diffraction gratings. Switching between multiple crystals is crucial for double-crystal monochromators. Appropriate mirrors and bandpass filters are used to remove higher-order harmonics. In cases where the range extends from the SX to HX regions, the beamline is equipped with two paths: one for a diffraction grating and the other for a double-crystal monochromator, with either path being utilized depending on the requirements of the experiment.

An example of a diffraction-grating monochromator covering a wide wavelength range is the design of the PF BL-19A/B [1]. BL-19A/B is a high-intensity beamline capable of utilizing energies ranging from 90 to 2 keV using a variable polarization undulator as the light source. A varied-line-spacing plane-grating monochromator is designed to cover a wide energy range using one grating. Furthermore, two types of gratings, 600 and 1200 l/mm, are available, which are designed to cover energy ranges of 75–1000 and 150–2000 eV, respectively, and are switched at approximately 650 eV for use. For higher-order harmonic suppression, a plain dispersion mirror with Cr, Ni, and Au stripes is used. Cr removes approximately half of the higher-order harmonics above 500 eV, Ni above 800 eV, and Au is used for wavelengths above 800 eV.

In the case of PF-HLS, owing to the high-brilliance design that enables the use of smaller beams, a multilayer grating with stepwise or continuous variation of groove spacing to control diffraction efficiency will be applicable and cover higher energy ranges. Well-designed diffraction gratings reduce the efficiency of secondary and higher-order diffraction, so that a single mirror can suppress higher-order harmonics. Double or triple mirrors will be used for more advanced suppression. The high-order harmonic suppression mirror system of the PF BL-12A is an example of a double mirror. Initially used in the previous BL-11A, this mirror system consists of a pair of flat Si mirrors positioned between the post-focusing mirror (M3S) and the focal point. The surface is half-coated with Ni, allowing for three selectable modes by translating the mirror: “without a mirror,” “Si mirror,” and “Ni mirror.” The incidence angle can also be adjusted from 1.5 to 10°, enabling efficient suppression of high-order harmonics [2]. A bandpass filter is utilized for energy regions of approximately 300 eV or lower, where mirror-based high-order harmonic suppression becomes inapplicable. For example, by using a 0.5-μm thick Al filter, third-order harmonics of 70 eV can be almost completely suppressed, making the range of 35–70 eV usable. For the ranges of 140–170 and 200–280 eV, Au and C filters with thicknesses of 0.2 and 2 μm are used, respectively.

Double-crystal monochromators can cover a wide energy range by switching between two types of crystals. For example, switching between Si(111) and Si(220) at approximately 20 keV can cover an energy range of approximately 2.1–70 keV, and Si(311) can be used for higher energies. The surface coating of mirrors is also effective for higher-order harmonic suppression in HX, with uncoated Si surfaces and stripes of Rh and Pt providing sufficient attenuation of higher-order harmonics in the aforementioned energy range. Considering the high brilliance of the PF-HLS, a practical-size mirror can be achieved even with a glazing angle of approximately 2 mrad for wide-wavelength-range utilization. Double mirrors will be used for a more advanced suppression.

The PF BL-12A is mentioned as an example of a beamline utilizing a wavelength range spanning SX to HX. BL-12A is designed to incorporate the functions of the previous BL-11A, -11C, and -11D, with the construction expected to be completed within fiscal 2023. By switching the first-stage mirror, either the grating or double-crystal monochromator can be selected, and by inserting or removing the final-stage mirror, a beam with a wide wavelength range of 50 eV to 5 keV can be irradiated at the same sample position (Figure 3-1-1). The PF-HLS is a high-brilliance machine; therefore, beam switching is expected to be more accessible. Future work on PF-HLS beamlines will focus on designing beamline optics, estimating radiation and thermal loads, and developing protective measures. Using the BL-12A, tests on the switching mechanism between the grating and double-crystal monochromators and evaluations of the performance of high-order harmonic suppression will be conducted to advance the experimental demonstration of wide-wavelength-range utilization.

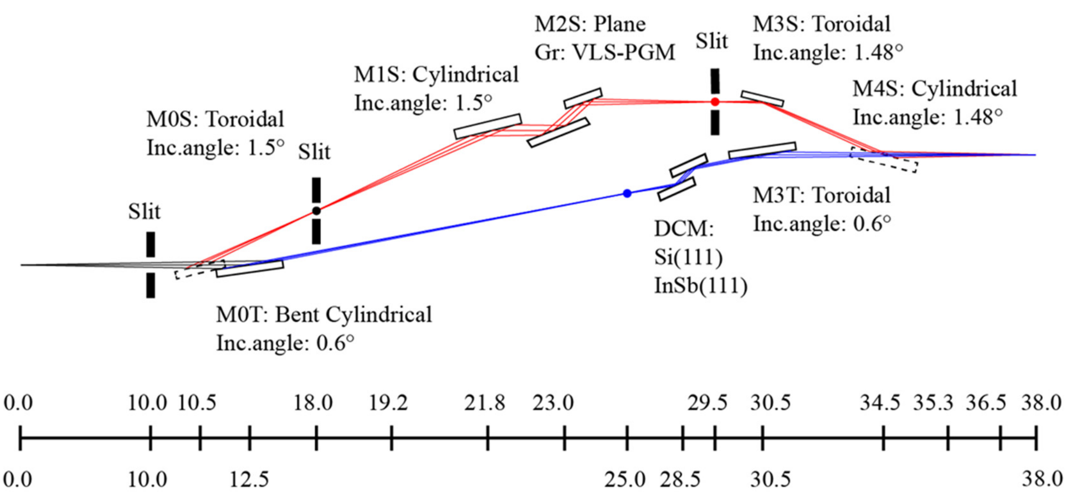

Figure 3-1-1: Layout (side view) of the wide-wavelength-range soft X-ray (SX) beamline BL-12A.

[1] https://www2.kek.jp/imss/pf/eng/apparatus/bl/bl19ab.html.
[2] Y. Kitajima *et al.*, *J. Electron Spectrosc. Relat. Phenom.* **101–103**, 927 (1999).

3-2. SR + SR Multibeam

At the PF-HLS, the multiple IDs placed in the straight sections of the storage ring enable the use of several high-brilliance beams (SR beams) in a single beamline. This section discusses the beamline technologies for the simultaneous use of two beams.

Figure 3-2-1(a) shows a grazing-incidence optics beamline with grating monochromators designed for the two-beam use in the SX region. From the IDs arranged in tandem, two beams are emitted with a directional difference of 1 mrad and are focused to approximately 10 μm and 50 nm, respectively, at the sample position. The simultaneous use of the two beams requires a precise adjustment of the focusing positions. In Figure 3-2-1(a), the focusing position of the high-focus beam is coarsely adjusted using the exit angle of the M3-SP mirror relative to the focusing position of the low-focus beam, followed by fine-tuning using a Fresnel zone plate (FZP). The two exit slits,

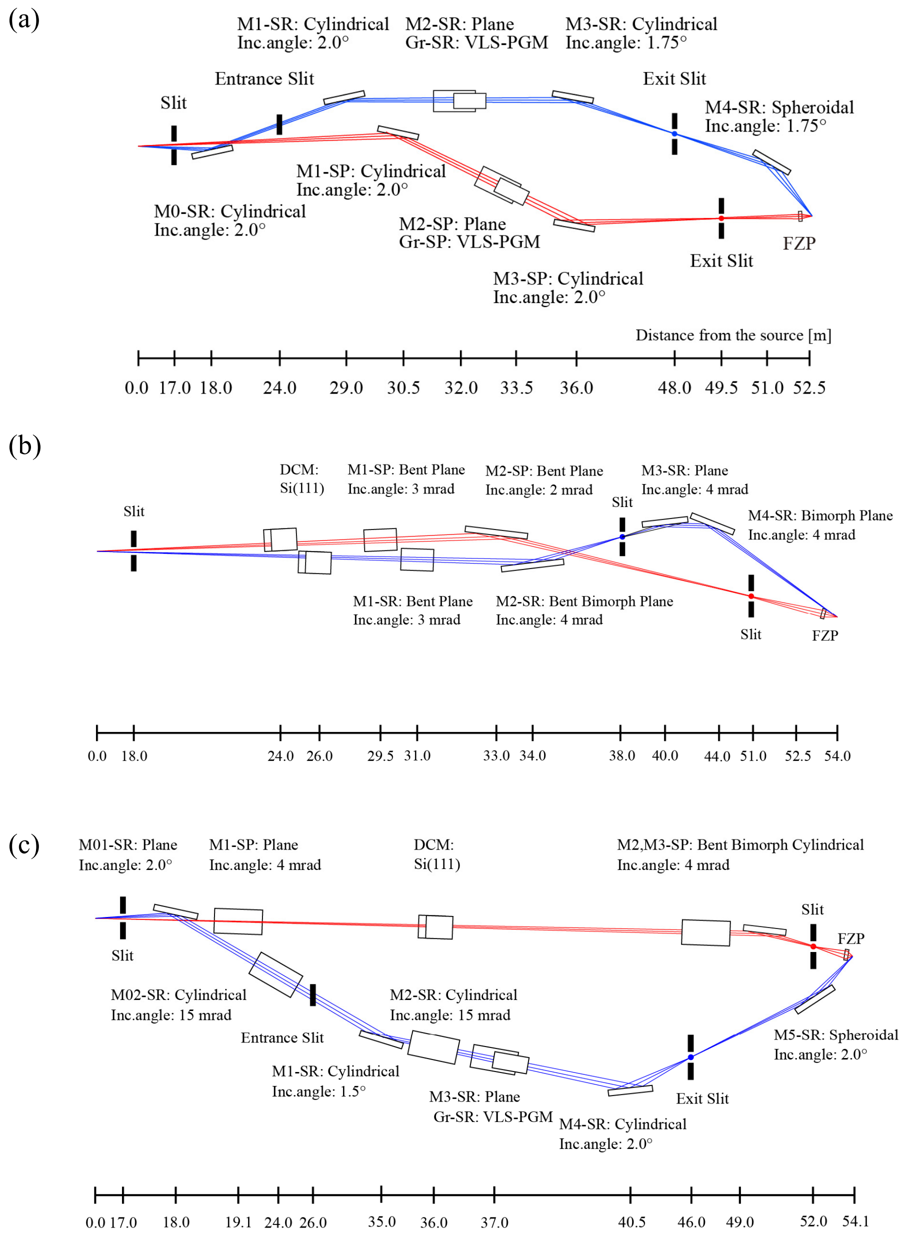

Figure 3-2-1: Examples of the beamline designs for the two-beam simultaneous use (plan view). (a) SX–SX, (b) hard X-ray (HX)–HX, and (c) SX–HX.

M4-SR mirror, and FZP are mounted on a single robust frame to prevent unintended relative movements of the two beams. Figure 3-2-1(b) illustrates the beamline design using two double-crystal monochromators for the two-beam use in the HX region. Compared to the SX example in Figure 3-2-1(a), the proximity conditions for the two beams are more stringent; however, this is achieved by the staggered placement of the monochromators and facing the horizontal mirrors opposite to each other. Owing to stricter requirements for the relative control of focused beams at the sample position, a meticulous design of the shape and placement of the final optical elements is necessary. Figure 3-2-1(c) shows the beamline design for the simultaneous use of SX and HX beams, where the SX beam is angled to align with the HX beam position.

In experiments using two beams simultaneously, precise control of the two beam positions is extremely important. Stable beam position control requires the detection and adjustment of beam positions and the stabilization of the light source and beamline optics. The white-beam position monitor (BPM) and the monochromatic BPM used for adjusting the beam position at the light source and sample location, respectively, should be appropriately positioned. Implementing a beam-position feedback system is crucial for controlling the beam positions. To stabilize the beamline optics, measures such as adopting static vacuum pumps, robust optical frames, thermal stabilization of optical elements, and stabilization of air conditioning inside the hutch are implemented. Furthermore, beam position control using a white two-beam position measurement system with a source feedback, testing of the suppression of interference between the two beams at the sample position, and control of the focused beams, are explored. The design and examination of the relative stabilization of beamline optics and experimental apparatus are also advanced.

The multifunctional research and development beamline PF BL-11A and -11B, which is currently under construction, is designed for the simultaneous use of SX and HX, although it uses a bending magnet source. This beamline will also be used to design and develop beam-position control mechanisms and conduct proof-of-concept experiments for the simultaneous use of two beams (Figure 3-2-2). In collaboration with PF-UA, UVSOR, and HiSOR, regular meetings and research sessions are held to advance various studies.

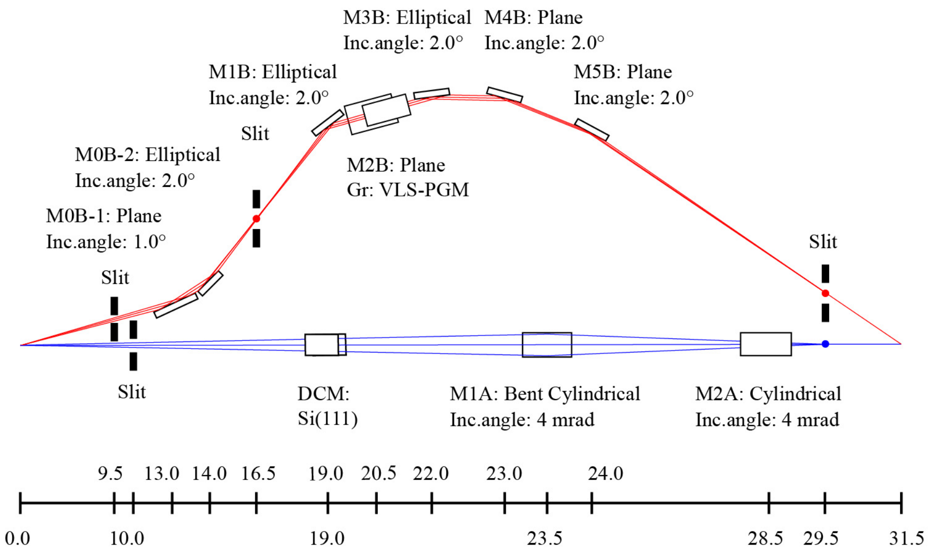

Figure 3-2-2: Layout (plan view) of the multifunctional research and development beamline BL-11.

3-3. SR + SP Multibeam

At the PF-HLS, in addition to the high-brilliance beam (SR beam) from the storage ring, the ultra-short pulse beam (SP beam) from the superconducting linac can also be used. This section discusses the beamline technologies for the simultaneous use of SP and SR beams.

A precise spatiotemporal control over the optical path length, irradiation position, and sample position on the beamline is required to conduct qualitatively different experiments using the high spatiotemporal resolution of the SP beam. The pulse width of the SP beam is 50–400 fs, and an SP beam controlled to a jitter of a few femtoseconds relative to the reference signal will be obtained. To utilize the short-pulse nature of the SP beam, the timing characteristics of the beamline and detectors are controlled to attain a jitter, drift, and deviation within 10 fs, which is equivalent to within 3 μm when converted into the light path. In beamlines that utilize timing information, the sample position must be reproducible with micron-level precision, particularly in the direction of light propagation.

A dedicated 250-bunch mode operation will be introduced to synchronize the two types of bunches, SP and SR. This implies adopting an operation mode for the SR beam, where one bunch is occupied every 50 buckets out of a harmonic number of 1250, thereby obtaining perfectly synchronized SP bunches. The superconducting linac will inject up to 1 nC × 6000 (microbunches) × 10 Hz (macrobunches). Although a 1 nC bunch is a significant charge, it is still insufficient to obtain a spectrum or diffraction pattern with just a few pulses, unlike free-electron lasers (FELs). Therefore, efficient signal accumulation methods are required. For example, in spectroscopy, dispersive XAFS-type measurements are performed by irradiating a white beam onto a sample and recording the transmitted absorption light [1]. In diffraction and scattering, the general method that irradiates a monochromatic light and records two-dimensional images of the diffracted or scattered X-rays [2] is employed.

For ultrafast time-resolved experiments using an SP beam as a probe (e.g., Science 2-5) or experiments using pump-and-probe schemes with SP and SR beams (e.g., Science 2-6), accurate recording of the time when the SP beam reaches the sample is crucial. The monitoring of time is conducted in two stages. For coarse adjustment, devices such as picosecond streak cameras or high-speed photodiodes combined with advanced digital lock-in amplifiers are prepared, which enables monitoring in the order of 10 ps. Devices with the required time resolution for visible and near-infrared lasers are commercially available and will be modified and improved for compatibility with synchrotron radiation. Next, for finer timing adjustments in the order of 10–100 fs, a monitoring method that uses fast photoinduced phenomena triggered by lasers will be established. The latest laser synchronization technology has achieved synchronization with less than 30 fs jitter relative to RF [3]. Therefore, by monitoring sufficiently fast photoinduced phenomena (such as in [4]) with SP and SR beams, the time can be recorded relative to the phase of the laser oscillation.

The changes in the optical path length due to the monochromator operation must be compensated to use the spectrally dispersed beam without changing its timing relative to the reference. In double-crystal monochromators for FELs, changes in the optical path length owing to the monochromator operation can affect time-resolved experiments, and mechanisms for correcting the optical path length to eliminate this influence have been realized [5]. For spectroscopic measurements utilizing the pulse characteristics of the PF-HLS, beamlines will be equipped with a mechanism to correct the changes in optical path lengths, including a high-precision surveying laser to measure the distances between optical elements within the monochromator. In diffraction-grating monochromators, the pulse length may be extended depending on the beam size in the dispersion direction of the grating [6]. The development of monochromators to suppress this extension will be conducted as required. A balance between the amount of light per pulse and the resolution must also be considered.

The time difference between the SP and SR beams is precisely controlled by the injection of the SP bunch. However, the optical path length for each beamline is different, and variations in time difference may occur depending on the experimental conditions and environments. Therefore, beamlines with mechanisms that change the optical path length must be equipped. This is achieved by constructing an optical chicane using four optical elements [7]. Developments will be made according to the properties of the light to be controlled, such as wavelength, pulse width, and light type (whether monochromatic or quasi-white). In addition, the development of mechanisms that do not alter the focusing characteristics when the optical path length is changed is essential.

[1] M. Katayama *et al.*, *J. Synchrotron Rad.* **22**, 1227 (2015); B. Abraham *et al.*, *J. Synchrotron Rad.* **26**, 629 (2019).

[2] T. Donath *et al.*, *J. Synchrotron Rad.* **30**, 723 (2023).

[3] H. Enquist *et al.*, *J. Synchrotron Rad.* **25**, 570 (2018).

[4] A.M. Lindenberg *et al.*, *Science* **308**, 392 (2005); A. L. Cavalieri *et al.*, *Phys. Rev. Lett.* **94**, 114801 (2005).

[5] Y. Kim *et al.*, *J. Synchrotron Rad.* **29**, 194 (2022).

[6] M. Brzhezinskaya *et al.*, *J. Synchrotron Rad.* **20**, 522 (2013).

[7] S. Roling and H. Zacharias, “Split-and-Delay Units for Soft and Hard X-Rays,” in E. J. Jaeschke et al. (eds.), Synchrotron Light Sources and Free-Electron Lasers (Springer Nature 2020).

4. Light-Source Accelerators

4-1. Overview

In the global research and development of light-source accelerators, many movements have been made toward fourth-generation light sources that aim to construct extremely low-emittance and diffraction-limited light sources, following the trend toward new third-generation low-emittance light sources. Conversely, we propose a light source that does not use emittance as the primary index but focuses on a light source that combines cutting-edge technology and versatility to realize a wide range of users' science. We aim to promote the following: 1) deepening of science by the wide energy-range SR beam beyond the new third-generation performance provided by the 2.5/5.0 GeV switchable storage ring, 2) fusion by the SR + SR two-beam (multibeam) utilization, and 3) creation using the high-performance SP beam from the superconducting linac. Carbon-neutral green transformation is an essential goal worldwide; therefore, research and development to reduce the construction and operation costs of light-source accelerators are indispensable. The PF-HLS is expected to reduce operation costs by 25–30% compared to the sum of the current PF and PF-AR. The parameters described in the following sections are preliminary and will be updated as necessary through future research and development.

The guidelines for the overall design are as follows: 1) a beam energy of 5.0 GeV is appropriate to provide photons in the high-energy region (~100 keV); 2) 2.5 GeV is desirable for the low-to-medium-energy region (VUV to SX); 3) considering the intensity of the synchrotron radiation, the light should be delivered principally from the IDs rather than the bending magnets, and 4) the emittance should be smaller than 1 nmrad at 5.0 GeV.

The magnetic field of the bending magnets should be as weak as possible to reduce power consumption during operation. Considering the distribution of synchrotron radiation facilities in Japan, the construction site should be located at the KEK Tsukuba Campus. Furthermore, carrying out the construction feasibly within the campus is essential. Based on these considerations, the circumference of the storage ring is selected as approximately 750 m. When launching the facility, a 2.5/5.0 GeV storage ring with an injector consisting of a normal-conducting linear accelerator (NCL) and booster ring (BR) will be constructed in advance, as shown in Fig. 4-1-1, to ensure a smooth transition of the users from the PF and PF-AR rings. Table 4-1-1 presents the parameters of the storage ring.

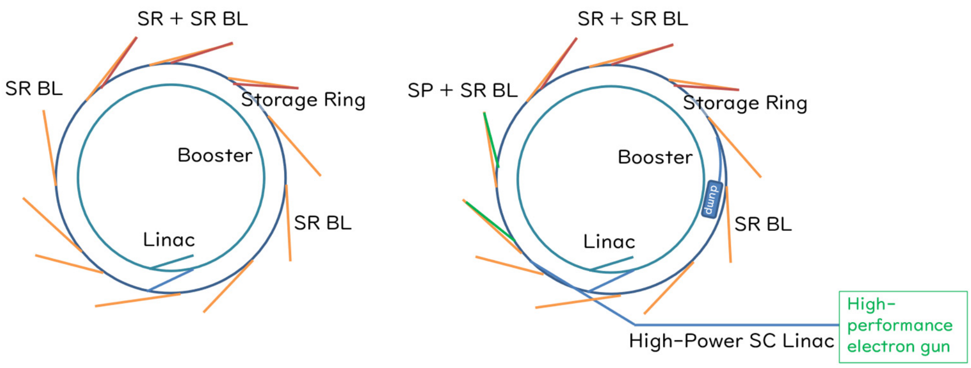

Figure 4-1-1: Conceptual diagram of the PF-HLS. The ring section will be constructed first (left), followed by the superconducting linear accelerator (right). In the first phase, a small linac and booster ring will be used for injection.

Table 4-1-1: Main parameters of the storage ring

Energy [GeV]	2.5	5.0
Circumference [m]	749.5	
Lattice structure	Double DDBA/8BA (modified)	
Number of normal cells	4	
Number of isochronous cells	11	
RF voltage [MV]	1.6	6.5
RF bucket height [%]	8.93	7.76
Radiation loss per revolution [MeV/turn]	0.222	3.557
Momentum compaction factor	3.24×10^{-5}	
Betatron tune, ν_x/ν_y	47.865/16.655	
Damping time, x/y/z [ms]	25.9/56.2/67.5	3.24/7.03/8.44
Stored current [mA]	500	200
Natural emittance [nmrad]	0.208	0.832
Energy spread	7.417×10^{-4}	1.48×10^{-3}
Natural bunch length	4.72 ps (1.4 mm)	7.21 ps (2.2 mm)
Touschek lifetime [h]	1.25 *	21 *

* XY coupling 1%, 1250 buckets fully filled

4-2. Lattice, Optics, and Beam Dynamics of the Storage Ring

In addition to the guidelines described in Section 4-1, a 2.5/5.0 GeV switchable storage ring for the PF-HLS has been designed considering the following conditions:

- The isochronous cells, through which the SP bunch passes, are arranged to suppress bunch lengthening.
- To conduct two-beam experiments in the VUV–SX region, maximum number of straight sections (10 m long) should be placed in the ring, at which two IDs of several meters will be installed with an orbit-switching system.
- To accumulate a high-charge isolated bunch, a magnet with minimal bore diameter will not be employed from the viewpoint of beam impedance. At present, we have limited the minimum bore diameter to 30 mm with reference to the current value used in the SOLEIL ring, which corresponds to 55 T/m for the upper limit of the quadrupole field gradient and approximately 6500 T/m^2 for the sextupoles. From the viewpoint of power efficiency, magnets will be utilized in a magnetic field region that is not highly saturated.
- To reduce the heat load due to synchrotron radiation in the vacuum system, the field strength of the bending magnets is weakened: 0.7 T at 5.0 GeV is targeted.

The aforementioned conditions concerning the magnetic fields considerably limit the optics design of a 2.5/5.0 GeV switchable storage ring for the PF-HLS as follows. The employment of the extremely low-emittance lattice, such as the multibend achromatic (MBA) lattice used in MAX IV and the hybrid MBA lattice used in ESRF-EBS, is difficult because of the limitation of the magnetic fields as mentioned above. The double-bend achromatic or triple-bend achromatic lattices used in the third-generation facilities would not provide sufficient emittance goal, even if the number of cells was increased. In the previous study on the conceptual design of the hybrid ring [1], we proposed a quadruple-bend achromatic lattice modified from the NanoTerasu lattice [2], which was considered the best solution for satisfying the aforementioned design conditions. The present PF-HLS lattice is further refined from the previous lattice by increasing the circumference from 350 to 750 m, the number of cells from 16 to 30, and the length of the straight section of every other cell

(a) (b)

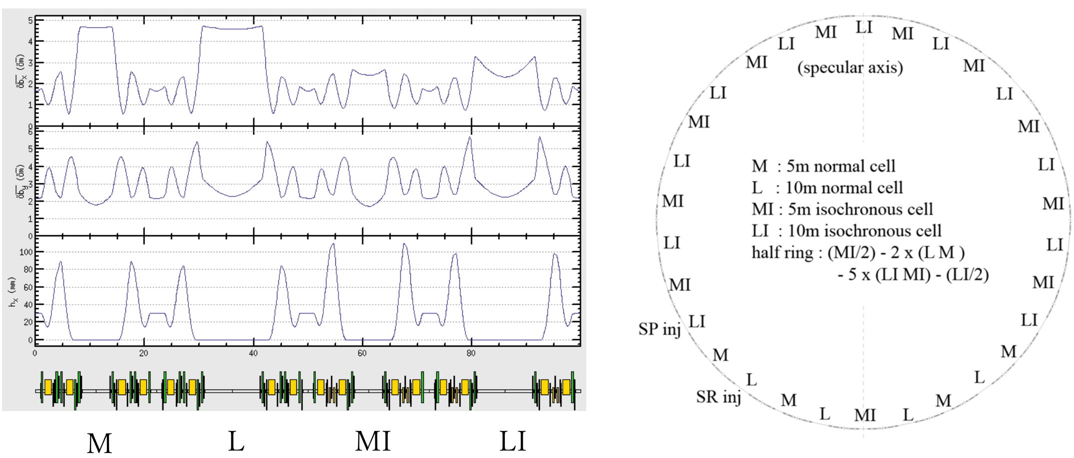

Figure 4-2-1: Ring lattices and optics. (a) Optics of the four basic cell types, (b) cell layout along the ring: M denotes a normal cell containing a 5-m straight section, L denotes a normal cell with a 10-m straight section, MI denotes an isochronous cell with a 5-m straight section, and LI denotes an isochronous cell with a 10-m straight section. Each cell contains a 2-m chromatic short straight section.

from 5 to 10 m. Consequently, the ring comprises four cell combinations: a normal cell with a 5-m straight section, normal cell with a 10-m straight section, and an isochronous cell for each, as shown in Figure 4-2-1. Every cell contains two dispersion bumps and a 2-m chromatic short straight section between them. The quadrupole magnets in the dispersion bumps of the normal cells are replaced with combined-function-type reversed-bending magnets to make the cells isochronous. In the case where the cell has a straight section of 10 m, changing both the quadrupole magnets inside the dispersion bump section from those used in the cell with a 5-m straight section is necessary to prevent an increase in emittance.

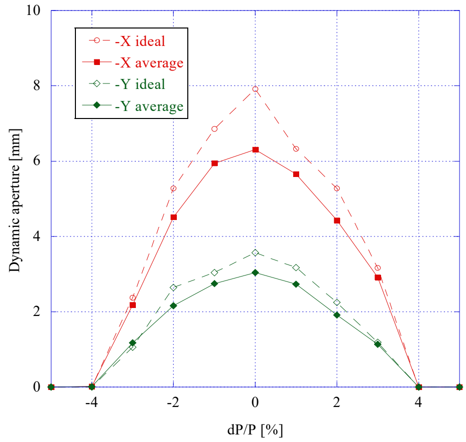

Figure 4-2-2: Dynamic aperture at the injection point.

For beam injection with the conventional system using kicker and septum magnets, a stable region of 5 mm is required in the horizontal direction at the injection point. Therefore, the sextupole field coefficients have been optimized by analytically correcting the resonant and amplitude-dependent tune shift terms [3]. The size of the stable region after COD conditions calculated for 100 different seeds is shown in Figure 4-2-2 with a standard deviation of 50 μm installation error, 0.05% magnetic field error, and 0.1 mrad rotation error in the XY coupling direction as random numbers up to ±1σ for the ring magnets. The stable region of 5 mm required for injection is shown to be secured.

Figure 4-2-3 shows the simulation results with the ELEGANT code [4] concerning the bunch lengthening and emittance growth, which are observed at the center of the long straight section of 10 m, for an SP bunch passing through the isochronous sections. The following initial SP bunch parameters are assumed: 0.1 nmrad emittance; 1 nC charge; 0.5% energy spread; and 50, 100, and 200 fs bunch lengths. An initial bunch length of 200 fs almost completely suppresses the emittance growth and bunch lengthening caused by coherent synchrotron radiation.

Impedances that cause beam instability or changes in the beam parameters are classified into two types: resistive impedances, which are mainly determined by the duct material; and geometric impedances, which are caused by the uneven duct structure. An accurate evaluation of the geometric impedances requires the design of each ring element. Assuming that only a suitable resistive impedance (e.g., ID vacuum chamber: aluminum; vertical aperture, 8 mm; total length, 180 m), the maximum growth rate of the bunch-coupled beam instability can be estimated to be approximately

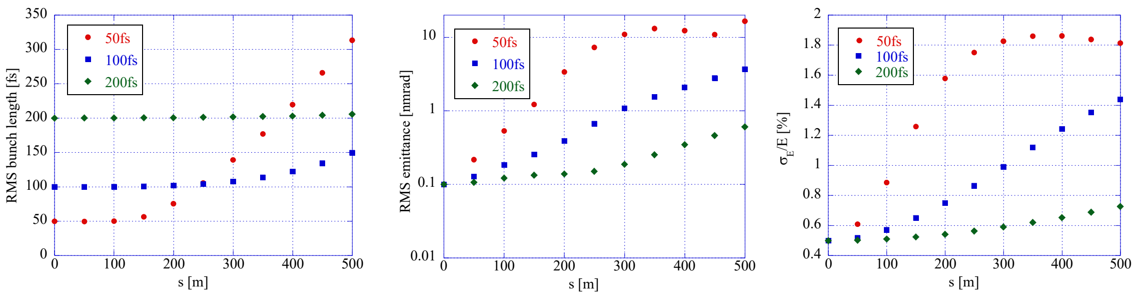

Figure 4-2-3: Temporal evolutions of RMS emittance (left), RMS bunch length (center), and energy deviation (right) of SP bunch passing along the central orbit of the isochronous cells.

$10000\ s^{-1}$ for a multibunch of 500 mA (0.4 mA × 1250 bunches). Therefore, a feedback system with an attenuation rate greater than $10000\ s^{-1}$ may eventually be required. In addition, because the momentum compaction factor is very small, the change in the beam spectrum due to chromaticity can be abrupt and induce higher-order mode instabilities with small positive values of chromaticity. The current threshold for the single-bunch vertical-mode coupling instability can be improved by decreasing the impedance or increasing the synchrotron tune. However, in a 2.5/5.0 GeV switchable storage ring, the latter countermeasure involving increasing the momentum compaction factor, radiation loss, and RF voltage is not as easy as it can be used in other light source facilities. Although enlarging the chamber aperture effectively reduces the impedance, widening the vertical gap between the undulators and magnets is challenging. The changes in the beam parameters and thresholds of the stored current will also be evaluated using simulations and theoretical analyses. The effects of the chromaticity and feedback should also be considered.

[1] K. Harada *et al.*, *J. Synchrotron Rad.* **29**, 118 (2022).
[2] N. Nishimori *et al*. *Proc. of IPAC2019*, 1478 (2019).
[3] Y. Shimosaki, *Proc. of PASJ2015*, 468 (2015).
[4] M. Borland, *APS LS-287*, September 2000.

4-3. Injection System

Regarding electron beam injection into the storage ring, realizing injection into the narrow dynamic aperture (5 mm) of the storage ring is essential, as well as achieving “transparent top-up injection” where the beamline users do not detect any decrease in brilliance or fluctuation of the optical axis. The PF was the first in the world to develop a scheme and realize injection using only one pulsed multipole magnet, and it has the advantage of having a negligible effect on the stored bunch. However, the conventional injection scheme using four bump magnets has advantages in terms of injection efficiency, stability, and reliability. Therefore, both systems are currently being considered for beam injection.

Figure 4-3-1 (top) shows the layout of the four bump magnets in the injection section of the storage ring, as well as the magnets on the injection-beam transport line. Beam injection from inside the ring is planned to avoid interference with the synchrotron radiation beamlines. Because an injection system using four pulsed magnets requires a high similarity in the magnetic field, an independent power supply is connected to each of the four magnets. The pulse power supplies for the pulse septum magnets, pulse multipole injection system, and counter kicker system will be equipped with solid-state switches. The introduction of solid-state switches will achieve a time jitter as short as several 10 ps and an output stability as high as less than 0.1%. A solid-state pulse power supply with a high repetition rate of 1 MHz is under development and will be used for bunch-orbit control.

Figure 4-3-1 (bottom) shows a schematic of the beam positions of the injection and stored bunches at 5.0 GeV operation. The horizontal beta function of the storage ring is 21 m. The design is such that the injection bunch is involved within a 5 mm area on one side of the dynamic aperture of the stored bunch. The standard bump-orbit height is 4 mm, but it can be raised up to 7.5 mm for on-axis injection during beam commissioning.

The following four requirements are the vital in realizing stable operation: (A) generation and transport of low-emittance injection bunches; (B) realization of various bunch-fill patterns, including high-charge isolated bunches; (C) injection of 2.5/5.0 GeV switchable energy electron bunches; and (D) two phases for beam injection, that is, injection with the combination of the NCL and the BR, and short pulse beam injection with the SCL.

In the first phase, the beam injector will consist of a 35 m long NCL and a 720 m perimeter BR. Low- and high-energy beam transport lines, NCL to BR (NCBBT) and BR to storage rings (BSBT), are also required. Figure 4-1-1 (right) shows the preliminary planned configuration of the injector,

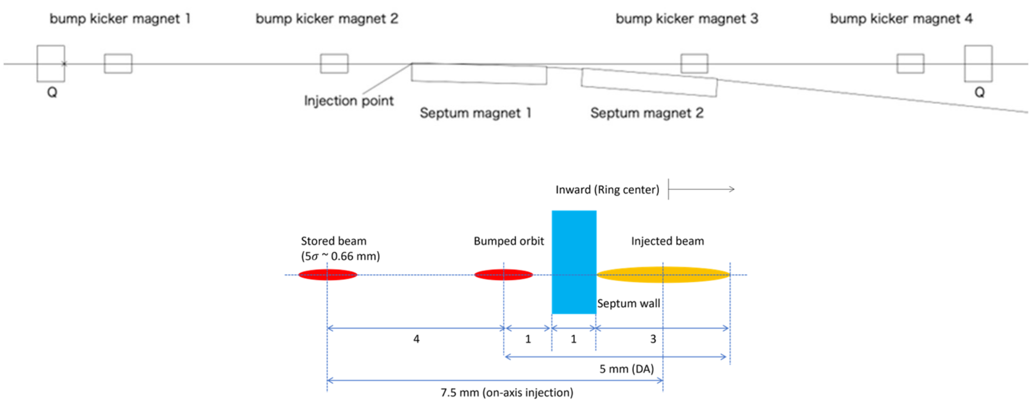

Figure 4-3-1: Injection system components in the injection section of the storage ring (top) and beam positions at the injection point (bottom).

including the future construction of the SCL. The layout of BSBT is also illustrated in Figure 4-3-2.

An NCL with a higher beam energy preferably suppresses beam instabilities, whereas an NCL with a lower energy is beneficial in terms of construction and operation costs. In addition, as the ramp-up scale (the ratio of the maximum beam energy to the NCL energy) increases, the hardware design, including power supplies, becomes more difficult; and some associated operational difficulties are anticipated. At present, an NCL with an energy of 250 MeV is considered with a charge of 1 nC, maximum repetition rate of 50 Hz, and normalized beam emittance of 5 μmrad. The BR is configured with a 60-cell FODO lattice using combined-function-type bending magnets. The booster and storage rings are considered to be installed in the same radiation-shielded tunnel for building cost considerations.

An SCL is planned for installation in an underground tunnel. The beam transport line connecting the SCL to the storage ring (SCSBT) adopts isochronous-magnet optics. The bunch from the SCL is injected into the storage ring, and after passing through two-thirds of the storage ring, the bunch is kicked out from the storage ring and dumped at the underground dump point (shown as "dump" in Figure 4-1-1). The connecting point of the BSBT should be separated from that of the SCSBT to enable the top-up operation of the storage ring without disturbing the user's SR + SP two-beam application.

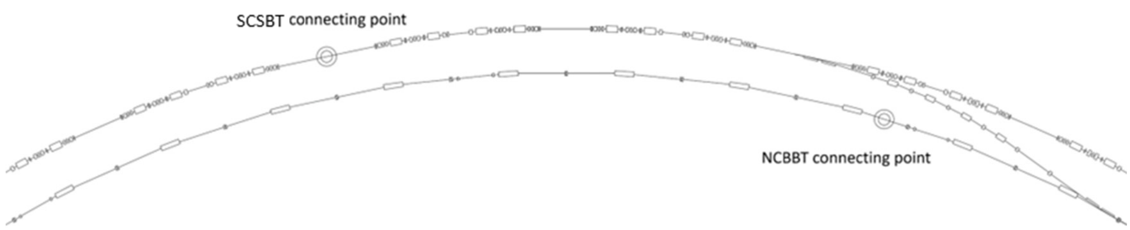

Figure 4-3-2: Schematic of the beam transport path connecting the booster ring to the storage ring.

4-4. RF Acceleration System

The key role of an RF acceleration system for a storage ring is to contain the energy fluctuation of the electron bunch owing to the quantum nature of synchrotron radiation and maintain the stability of the longitudinal motion of the circulating bunch. The basic configuration of an RF system is shown in Figure 4-4-1. An RF signal derived from the master oscillator is input to a low-level RF control (LLRF) system. The amplitude and phase of the cavity RF voltage are precisely controlled using a feedback controller built into the LLRF system. The LLRF system is also pivotal in protecting RF equipment by rapidly switching off the RF output signal in the event of an anomaly. Next, an RF amplifier amplifies the low-level RF signal to the 100 kW level. The amplified RF signal is guided to the RF cavity through a high-power RF transport system with a circulator and dummy load to separate and dump the reflected RF signal from the cavity. A semiconductor amplifier or klystron is used as the RF amplifier.

In addition to conventional issues, the following issues must be considered to realize the SR + SP multibunch and 2.5/5.0 GeV energy-switching operations of the storage ring, which are the features of the PF-HLS:

a) Selection of the SR frequency to realize the synchronization with the SP bunch

b) RF system capable of stable bunch operation at both 2.5 and 5.0 GeV energies

The relaxation of the intrabeam scattering effect is another issue, particularly for the uniform filling mode and time-resolved mode (isolated single/several-bunch filling) at low energy (2.5 GeV). Therefore, the following is also required:

c) Bunch-lengthening system that simultaneously achieves a stable beam operation and sufficient lengthening performance in various operating modes.

In this section, the basic policy for the aforementioned three issues of the RF system is described individually, along with the current status of the PF.

<u>a) Selection of the SR frequency to realize the synchronization with the SP bunch</u>

In the case that both SR and SP beams are delivered to a certain beamline, SR beams arrive at intervals corresponding to the storage-ring RF frequency and the bunch-filling pattern, and SP beams arrive continuously for approximately 0.6 ms (macropulses) at integer multiples of the intervals corresponding to the SCL RF frequency. These SP and SR beams can be synchronized by appropriately selecting the SCL RF frequency, storage-ring RF frequency, and harmonic number of the storage ring.

Regarding the frequency selection of the SCL, the RF frequency is selected as 1.300 GHz to fully utilize the technology developed in the Linear Collider project. For the PF ring and PF-AR, the RF frequencies are in the 500-MHz band (500.1 MHz and 508.6 MHz, respectively), and effectively using these existing RF-related resources is desirable. Based on these considerations, the RF frequency of the storage ring is selected as 500.0 MHz. In this case, considering that the harmonic number of the storage ring is 1250, all SP bunches in the macropulse can be synchronized

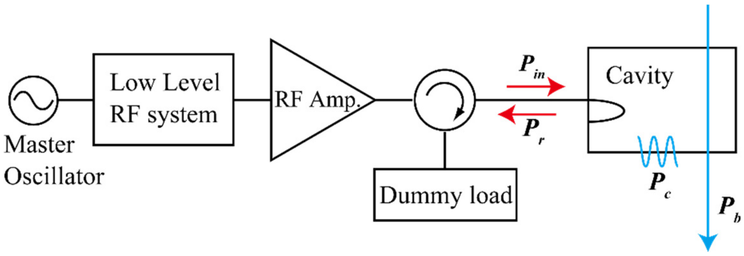

Figure 4-4-1: Basic configuration of the RF acceleration system.

with SR bunches by injecting SP bunches at micropulse repetition rates of 2, 4, 10, 20, 50, and 100 MHz. Here, the 4 MHz case is an operation mode in which 10 bunches are stored in the ring at 125 bucket (250 ns) intervals, corresponding to the conventional isolated bunch operation.

A phase stability of 0.02–0.05° can be achieved in a 500-MHz RF system if a digital feedback system is constructed using the current technology, and the time jitter of the SR beam is estimated to be 100–300 fs. When either RF frequency is shifted by 0.1 Hz, a time difference of 100 fs is observed between the SP and SR beams at a time corresponding to 0.5 ms of the macro-pulse.

b) RF system capable of stable beam operation at both 2.5 and 5.0 GeV energies

To construct an RF system for both energies of 2.5 and 5.0 GeV, the RF voltage required for 5.0 GeV operation can be excited in several located RF cavities, and the resonant frequency of the acceleration mode is shifted (detuned) for the RF cavities that are not required for the 2.5 GeV operation and placed in the “standby” mode. The impedance of harmful parasitic modes (i.e., higher- and lower-order modes) of all the placed RF cavities contributes to the coupled-bunch instabilities (CBIs) even in the 2.5 GeV operation. To suppress the CBI, we first consider the introduction of a well-designed damped cavity and different RF designs to spread the resonant frequency of the parasitic modes.

From the perspective of power conservation, technology selection should balance the seemingly conflicting phenomena of significant variations in RF output power for two different energies: smooth operation-mode switching and ease of maintenance.

c) Bunch-lengthening system that simultaneously achieves a stable beam operation and sufficient lengthening performance in various operation modes

Harmonic cavities that are robust to the fast transient beam load formed according to various bunch-filling patterns should be used to achieve a stable beam operation and sufficient lengthening performance in various bunch-filling patterns simultaneously. Therefore, a harmonic cavity with low R/Q and high Q is suitable. In addition, we consider the use of an advanced RF voltage control system consisting of a dedicated LLRF controller and kicker cavity.

4-5. Vacuum System and Beamline Front-End

In general, the vacuum systems of light-source accelerators are designed to have highly effective pumping speeds and low outgassing rates caused by photon-stimulated desorption (PSD) under various constraints to ensure a sufficiently long electron beam lifetime. The basic design principle is to achieve an ultrahigh vacuum of approximately 10^{-8} Pa.

Vacuum chambers must possess various characteristics, such as absorption of synchrotron radiation heat load (high thermal conductivity and durability), low impedance (high electrical conductivity and continuity of the inner profile), transparency against static magnetic fields (nonmagnetic), transparency against pulsed magnetic fields (low electrical conductivity), radiation shielding (high mass absorption coefficient), high workability (such as welding, forming, and accuracy), and other properties [1].

In addition, the PF-HLS vacuum system will be subjected to the following requirements: 1) 2.5/5.0 GeV switchability, 2) accommodation of SP bunches with high-charge isolated bunches and short bunch length, 3) small aperture (<30 mm) for a low-emittance lattice, 4) two radiation paths for a single beamline, and 5) particle-free (ultraclean vacuum) in the superconducting cavity.

Different considerations will be necessary for different beam energies. At 2.5 GeV, beam instability, short bunch length, and short Touschek lifetime must be carefully considered; the impedance effects become more pronounced, and the system must be operated at lower pressures to reduce gas-scattering and ionization effects. At 5.0 GeV, coping with the high power and energy of synchrotron radiation is necessary; thus, the vacuum system must have high heat-load absorption and radiation-shielding properties.

In the design of vacuum chambers, considering the more severe heat-load conditions at 5.0 GeV, the antechamber structure, which can separate the electron beam path from the synchrotron radiation path, is the most likely candidate. Oxygen-free copper is a good candidate as a chamber material, considering the above requirements and physical properties.

An important performance indicator in the operation of a light-source vacuum system is the speed at which the design pressure can be reached by a photon-scrubbing operation during commissioning. The prediction of vacuum surface conditioning is performed by a 3D Monte Carlo simulation of Synrad and Molflow [2], using the PSD data of various vacuum surfaces measured at the PF BL-21 (Figure 4-5-1). Non-evaporative getter coatings, which have been studied and developed at the PF, are the most promising candidates for inner surface coatings with low PSD characteristics and high effective pumping speeds [3].

The part of the storage ring that directly connects the vacuum system to the synchrotron beamline is known as the beamline front end or beam channel. This part is essential to properly handle extremely and sharply directed synchrotron radiation generated from various light sources, such as

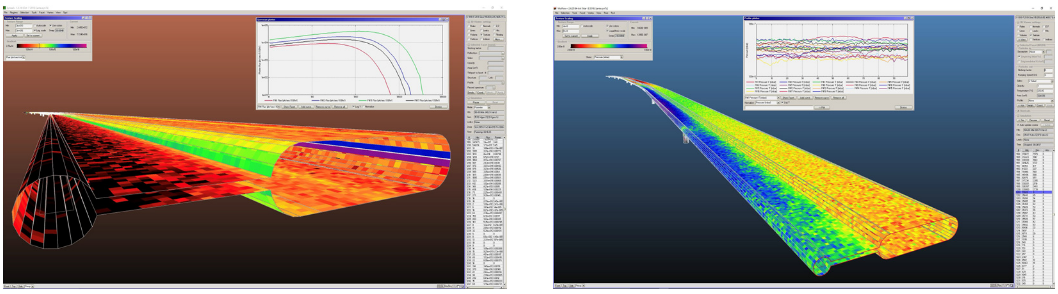

Figure 4-5-1: Example of a Synrad and Molflow-combined simulation for vacuum chambers with an antechamber structure.

bending magnets and insertion devices. A photon shutter, assembled using a water-cooled copper block, prevents vacuum accidents by absorbing the heat load concentrated in a narrow area. The photon shutter is designed for the 5.0 GeV operation, which has a high heat load and can be used for the 2.5 GeV operation.

In addition, water-cooled masks will be installed at several locations in each beamline front end to collimate the synchrotron radiation to the size required by users. A radiation-shielding shutter called the Safety Shutter will be installed at the downstream end of the front end, which consists of a stainless steel or heavy-metal block made mainly of tungsten that moves up and down in an ultrahigh vacuum. In the case of vacuum deterioration downstream of the beamline, the gate valve is closed rapidly to prevent vacuum deterioration from affecting the light-source accelerator, thereby ensuring stable operation. The machine protection system described above is independent of the personnel protection system, which is installed separately. However, information of both the systems must be coordinated appropriately.

[1] Y. Tanimoto, Vacuum Technology for Advanced Light Source Accelerators, OHO'15 Text.
[2] R. Kersevan and M. Ady, Synrad and Molflow Development, https://cern.ch/molflow.
[3] For example, X. G. Jin, Y. Tanimoto, T. Uchiyama. T. Honda, *Vacuum* **207,** 111671 (2023).

4-6. Beam Diagnostic and Control System, Accelerator Control System

To fully utilize the excellent performance of the PF-HLS and realize stable operation as a synchrotron radiation source, a beam diagnostic system that can precisely measure various parameters of the circulating bunches and a beam control system that stabilizes the beam orbit and maintains an arbitrary filling pattern are essential. An accelerator control system that remotely controls and monitors accelerator components is another important element of the PF-HLS. In this section, we describe the beam diagnostic and control system of the PF-HLS, as well as the components necessary for accelerator control.

Beam diagnostic system

Beam position monitors (BPMs) with four button-type electrodes will be used to measure the beam orbit. In addition to the BPMs for fast orbit feedback, approximately 20 BPMs will be installed for multipurpose applications. MicroTCA.4-based circuits developed for the PF ring will be upgraded and employed for the signal processing of the BPMs. The stored ring current will be measured using a commercially available DC-beam current transformer integrated into a dedicated vacuum chamber with a ceramic break. The beam loss rate and its distribution will be measured by distributing beam loss monitors, which combine scintillators and photosensors, along the ring. A dedicated beamline for beam diagnostics using a bending magnet or multipole wiggler as a light source will be constructed, and synchrotron radiation monitors using X-ray and visible-light components will be installed. The beam size will be measured using an X-ray pinhole camera and a visible-light interferometer. This will be utilized to evaluate the emittance and energy spread of the stored bunch. For measuring the bunch length, a synchro-scanning visible light streak camera can be used for stored beams above a few ps, whereas for single-pass bunches on the order of 50 fs to sub-ps, a deflecting cavity or an electro-optic sampling method is being considered. The bunch purity in the single-bunch and hybrid operation modes will be measured using a time-correlated single-photon counting method with an avalanche photodiode. X-ray BPMs with four tungsten blades will be installed in every undulator beamline and used for precise adjustment and stability measurement of the optical axis. Betatron tune of the ring is measured using the above BPM signal and a stripline-type kicker to shake the stored beam. Other beam diagnostic methods specific to the PF-HLS, where SR and SP bunches coexist, include beam position measurement using the difference in repetition frequency and bunch length of each bunch and single-pass beam profile measurement using a screen monitor equipped with an RF shield.

Beam control system

Orbit fluctuations with a period longer than 10 ms, which are mainly caused by the mechanical vibration of the magnet girders due to air conditioning, cooling water, and vacuum pumps, in the accelerator room and by the output ripple of the magnet power supply will be suppressed by fast orbit feedback using 10-kHz rate data from the BPM signal processing circuits. Fast orbit fluctuations on the order of a few microseconds due to beam instability and injection will be suppressed by the bunch-by-bunch feedback, which can detect the oscillation at each bunch and attenuate it at each turn. A commercially available dedicated circuit that has been empirically verified in the PF ring will be used for digital signal processing of the feedback. As a fast kicker is used to kick the beam for each bunch, stripline- and cavity-type kickers will be developed and used in the transverse and longitudinal directions, respectively.

The filling pattern of the ring is measured by inputting the BPM signal into a wide-bandwidth oscilloscope or similar device, and the bunch with the smallest charge compared to the target pattern is selected from the waveform data obtained for one revolution. An arbitrary filling pattern can be obtained and maintained by feeding back this bunch address to the injector at a period shorter than the beam-injection interval.

The bunch purity is maintained below 10^{-6} by constantly purifying several tens of buckets behind the isolated bunch. Purification is performed by amplifying an RF knockout signal gated synchronously with the revolution of the isolated bunch using a broadband RF amplifier and applying it to a dedicated stripline-type kicker.

Accelerator control system

The Experimental Physics and Industrial Control System (EPICS), which has been used in many accelerator facilities, including the PF ring, will be employed as an accelerator control software suite. EPICS is a network-distributed control framework that controls various devices connected to a network using a standard protocol called Channel Access. In contrast, the Simple Transmission and Retrieval System (STARS) developed in the PF ring will be used to control the beamline equipment, and EPICS and STARS can be mutually controlled via a gateway. The control hardware will be based on a programmable logic controller, and when high-speed control is required, it will be appropriate to use a MicroTCA.4 standard control board, which has been developed for BPM signal processing circuits.

For the control network, the policy is to select the most appropriate technology and products during the construction phase, and the bandwidth should be at least 10 Gbps for the backbone and 1 Gbps for the edges. Security is a critical topic, and appropriate firewalls and gateway devices will be installed between the network and other networks to realize secure and convenient internetwork communication. The archiver appliance will automatically store and retrieve various data, including the accelerator-operating parameters. The data can be easily retrieved, displayed, and analyzed using a dedicated application or standard web browser.

4-7. Insertion Device

An important goal of the PF-HLS is to switch the stored energy between 2.5 and 5.0 GeV, whereby a wide wavelength range of synchrotron radiation from a single ID will be available. High-brilliance light in a wide wavelength range from 10 eV to 100 keV will also be available by arranging IDs in tandem in a single straight section. Because the use of an ID with this large energy switch between 2.5 and 5.0 GeV is unprecedented worldwide, the concept should differ from the design of conventional insertion devices for high-brilliance rings. In a single-energy ring, the parameters of the ID are optimized to achieve the highest brilliance in the required wavelength range and polarization conditions by fully utilizing the straight section for the ID. In contrast, in the PF-HLS, the parameters must be adjusted such that no gap exists in the wavelength range when switching the electron energy while sufficiently suppressing the radiation power of the insertion device when operating at 5.0 GeV. Considering the aforementioned, we have examined the ID parameters assumed for the PF-HLS.

For the X-ray light source, a 20-mm periodic in-vacuum undulator will be employed, in which a wide wavelength range from 1 to 100 keV is targeted by using up to 15th-order light. The minimum gap is assumed to be 4 mm, which is the same as that of the short-period undulators in the PF ring. For a VUV–SX light source, a variable-polarization undulator will be fully utilized, with the APPLE-II type and the 6-row type, both of which have been well developed at the PF ring in accordance with the wavelength range. The PF-HLS will not use circular orbit radiation from bending magnets but will use relatively short multipole wigglers (MPWs) and 3-pole wigglers in short straight sections to utilize synchrotron radiation. By significantly switching the energy of the ring, the ring can be used as a light source in the high-energy region without using a significantly strong magnetic field. Below are the ID parameters currently under consideration and examples of their spectra.

Table 4-7-1: Undulator parameters

Synchrotron radiation range	ID type	Periodic length	K-value	Minimum gap	Total length	Wavelength range
X-ray	In-vacuum	20 mm	2.1	4 mm	1~4 m	1~100 keV
VUV–SX	EPU (APPLE-II type)	56 mm	4	12 mm	<5 m	200 eV~15 keV
VUV–SX	EPU (6-row type)	160 mm	7.6	12 mm	<5 m	10 eV~5 keV

Table 4-7-2: MPW and 3-pole wiggler parameters

ID	Type	Periodic length	Polarization	Minimum gap	Total length	Maximum magnetic field	Orbital amplitude @2.5 GeV
MPW	In-air	120 mm	V/H	12 mm	~0.5 m	>1 T	~50 μm
	In-vacuum	120 mm	V/H	4 mm	~0.5 m	<2 T	~100 μm
	Superconducting	80 mm	V	40 mm	~0.5 m	~3 T	~60 μm
3-pole W	In-air	150 mm	H	<20 mm	<0.3 m	~1 T	~100 μm
	Superconducting	350 mm	V	50 mm	<0.3 m	5 T	5 mm

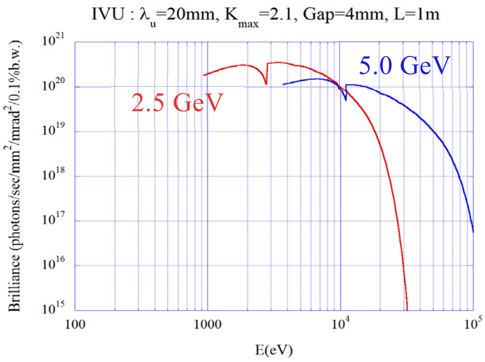

Figure 4-7-1: Spectrum examples of an X-ray source. (Red: 2.5 GeV, Blue: 5.0 GeV similarly hereafter)

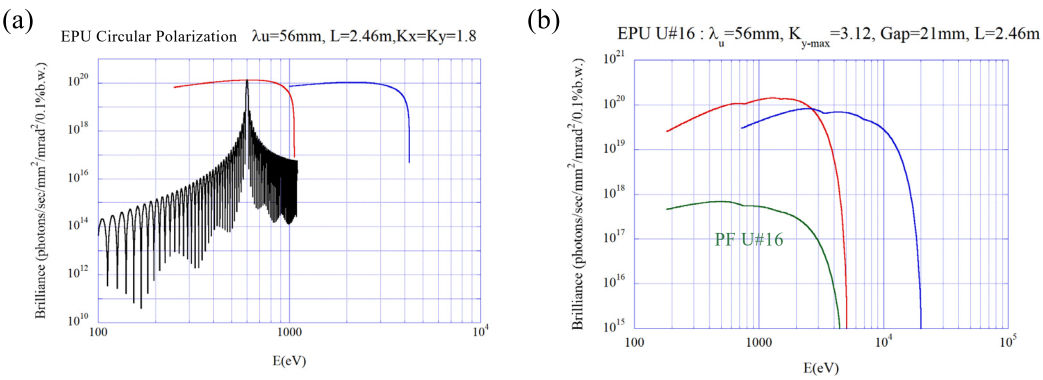

Figure 4-7-2: Spectrum examples of VUV–SX source 1, the APPLE-II-type variable polarization undulator. (a) Circular polarization mode and (b) linear polarization mode

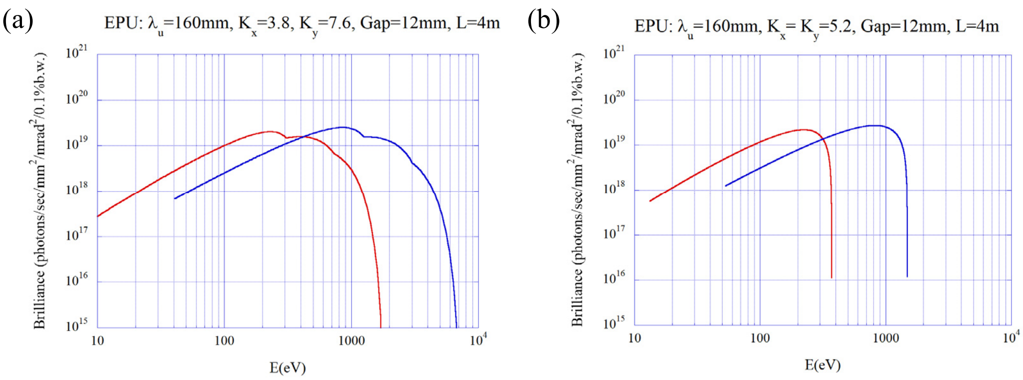

Figure 4-7-3: Spectrum examples of VUV–SX source 2, the 6-row-type variable polarization undulator. (a) Elliptical polarization mode (Bx/By = 1/2) and (b) circular polarization mode (Bx/By = 1)

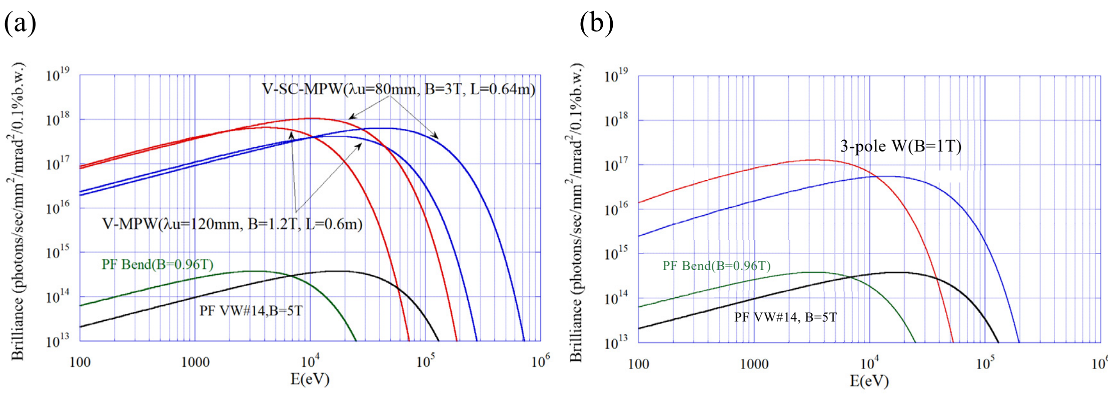

Figure 4-7-4: Spectrum examples of (a) MPW and (b) 3-pole W. (Compared to PF Bend and VW#14)

4-8. Superconducting Linear Accelerator

This section describes the SCL used as the light source in the PF-HLS. An overview of the accelerator layout is shown in Figure 4-1-1. Table 4-8-1 lists the parameters of the SCL described in the hybrid ring paper [1]. Although these parameters are based on the design at a beam energy of 3.0 GeV, the scale is approximately the same as that for the PF-HLS 2.5 GeV SCL, and only the bunch repetition rate within the macropulse, assuming a bunch charge of 1 nC, has been changed from 18 to 10 MHz.

These parameters are investigated based on International Linear Collider (ILC) specifications, some of which differ from the performance requirements of the PF-HLS. For example, owing to differences in beam patterns (bunch structures/configurations) and charges, a dedicated beam source (electron gun and laser) must be developed. The power coupler to feed the RF power into the acceleration cavity is another component that must be developed, owing to the differences in the average current and the amount of charge in the macropulse. The required specifications for the beam dump are also different from those of the ILC design, and a dedicated design for the PF-HLS is necessary. We will continue to conduct further research and develop these items.

Table 4-8-1: Long-pulse SCL parameters

Electron beam parameters	
Energy [GeV]	3
Average current [mA]	0.1
Bunch charge [nC]	1
Normalized emittance [μmrad]	0.6
Natural emittance [nmrad]	0.1
Bunch length [fs]	50
Energy spread [%]	0.5
Accelerator parameters	
RF frequency [GHz]	1.3
Acceleration gradient [MV/m]	30
Number of 9-cell acceleration cavities	96
Number of cryomodules	12
Macro-pulse repetition frequency [Hz]	10
RF macro-pulse width [ms]	1
Flat top width in macro-pulse [ms]	0.6
Number of bunches per macro-pulse	10000
Bunch repetition frequency in macropulse [MHz]	18
RF heat load per cryomodule (2K) [W/module]	8
Static heat load per cryomodule (2K) [W/module]	8
Required chiller capacity (2K) [W]	200

[1] K. Harada *et al.*, *J. Synchrotron Rad.* **29**, 118 (2022).

Photon Factory （Mar. 2024）
E-mail: photon.factory@kek.jp
https://www2.kek.jp/imss/pf/pf-hls/